Article

Mechanical Properties of Polyamide Fiber-Reinforced Lime–Cement Concrete

Mohammad Mostafa Jafari [1], **Soheil Jahandari** [2,3], **Togay Ozbakkaloglu** [4], **Haleh Rasekh** [5], **Danial Jahed Armaghani** [5,*] **and Aida Rahmani** [2,3]

1. Department of Civil Engineering, Technical and Vocational University (TVU), Tehran 1435761137, Iran; jafari-moh@tvu.ac.ir
2. Chem Concrete Pty Ltd., Seven Hills, NSW 2147, Australia; soheil@chemconcrete.com.au (S.J.); aida@chemconcrete.com.au (A.R.)
3. Centre for Infrastructure Engineering, Western Sydney University, Penrith, NSW 2751, Australia
4. Department of Civil Engineering, Texas State University, San Marcos, TX 78666, USA; togay.oz@txstate.edu
5. School of Civil and Environmental Engineering, University of Technology Sydney, Sydney, NSW 2007, Australia; haleh.rasekh@uts.edu.au
*   Correspondence: danial.jahedarmaghani@uts.edu.au

Abstract: Lime–cement concrete (LCC) is a type of lime-based concrete in which lime and cement are utilized as the main binding agents. This type of concrete has been extensively used to construct support layers for shallow footings and road backfills in some warm regions. So far, there has been no systematic research conducted to investigate the mechanical characteristics of polyamide fiber-reinforced LCC. To address this gap, LCC specimens were prepared with 0%, 0.5%, 1%, and 2% of polyamide fibers (a synthetic textile made of petroleum-based plastic polymers). Specimens were then cured for 3, 7, and 28 days at room and oven temperatures. Then, the effects of the fibers' contents, curing conditions, and curing periods on the mechanical characteristics of LCC, such as secant modulus, deformability index, bulk modulus, shear modulus, stiffness ratio, strain energy, failure strain, strength ratio, and failure patterns, was investigated. The results of the unconfined compressive strength (UCS) tests showed that specimens with 1% fiber had the highest UCS values. The curing condition and curing period had significant effects on the strength of the LCC specimens, and oven-cured specimens developed higher UCS values. The aforementioned mechanical properties of the LCC specimens and the ability of the material to absorb energy significantly improved when the curing period under the oven-curing condition was increased, as well as through the application of fibers in the mix design. Based on the test results, a simple mathematical model was also established to forecast the mechanical properties of fiber-reinforced LCC. It is concluded that the use of polyamide fibers in the mix design of LCC can both improve mechanical properties and perhaps address the environmental issues associated with waste polyamide fibers.

Keywords: lime-based concrete; mechanical characteristics; fiber reinforcement; curing conditions; curing periods

1. Introduction

Soil stabilization is a common method for improving mechanical properties, enhancing stability, and reducing the lateral deformation and settlement of soil [1–4]. Depending on the thickness of a soil layer, different stabilization methods can be adopted, including pre-loading, the use of chemical stabilizer additives, soft deposit replacement and removal, stone columns, surface mattresses, lightweight fills, surcharge loading, and control of compaction. However, some of the materials used in the treatment are costly and ineffective [4,5]. For example, replacement and removal, control of compaction, surcharge loading, and column of stone are somewhat costly. Meanwhile, the addition of gypsum is often

found to be ineffective [6,7]. Consequently, new methods have emerged to deal with soil problems, aiming to enhance strength and decrease swelling behavior.

Lime stabilization is an attractive method for improving the properties of clayey soils. The main application of lime, as a well-established method in the construction industry, is the stabilization of problematic soils such as expansive soils, collapsible soils, and soft clays [8,9]. Lime concrete (LC), lime-stabilized soil, lime–hemp concrete, lime mortar, lime–cement concrete (LCC) have been used in various construction sites; however, the sample preparation process and their applications make them very different from each other [10–15]. In the lime application for construction projects, the clay soil, lime, and water are compacted using a roller after being mixed well. Improving the rail tracks and pavement layers are among the main applications of this method [7,16]. Another lime application is lime mortar, which is used to bond masonry blocks [17,18]. To make lime blocks, lime–hemp concrete is manufactured using water, clay, lime, hemp, and coarse aggregates [19,20].

Various studies have reported on the feasibility of using lime as a clay soil stabilizer. Because of the strong pozzolanic reaction between lime and soil, the treatment can reduce the plasticity index, increase the unconfined compressive strength (UCS), and control the swelling potential [21]. For example, Bartlett and Farnsworth [22] concluded that soil stabilized with LCC has a lower initial settlement by about 0.8 m in the stabilized area in comparison with the untreated area. Rogers et al. [8] concluded that the use of lime improves the resilient modulus and strength of the soil and that the addition of lime and cement can significantly reduce the plastic strain. Chand and Subbarao [23] reported that specimens stabilized with 14% lime cured for 180 days had higher UCS, rebound hammer numbers, slake durability, and point load strength index scores compared to specimens treated with 10% lime at different curing times. The study by Malekpoor and Toufigh [24] showed substantial growth in the load-bearing capacity of soft soil improved with LC columns containing 20% lime and 22% clay and a substantial strength reduction while in a saturated condition. Toohey et al. [25] reported that the UCS results for the specimens cured at 23 °C for 28 days were lower compared with those cured at 41 °C for 7 days.

The use of lime in soil stabilization and the production of LCC results in improved mechanical properties and reduced swelling potential and ductility. Adding fibers to the mix design of LCC and lime-stabilized soils is considered to be a cost-effective and environmentally friendly method to improve ductility performance [26]. Fibers have a wide application in various fields of engineering [27–29]. The application of fibers as soil reinforcement with or without cement has been reported previously [30–36]. Miraftab and Lickfold [35] reported that, in recent years, many waste producers have sought to utilize waste fiber products to improve the performance of various materials. Improving the mechanical properties of soils with the addition of fibers can reduce the required cement content. Mandal and Murti [37] found that a mixture of soil and high-tensile-strength fibers can improve the engineering characteristics of soil.

In recent decades, various natural fibers such as coconut fibers [38], sugarcane [39], sisal [40], hemp [41], and palm fiber [42] have been used for soil reinforcement. In many cases, synthetic fibers have also been used for this purpose. Among the different types of synthetic fibers used for soil reinforcement, polyethylene fiber [42,43], polyester [44,45], glass [44,46–48], carbon [49,50], and iron [51] can be mentioned. But, it is important to pay attention to the fact that, despite the cheapness and better ductility of natural fibers compared to synthetic fibers, they have much less resistance to atmospheric conditions and environmentally corrosive factors, especially compared to polymer synthetic fibers [52]. The use of polyamide fibers, as a synthetic textile made of petroleum-based plastic polymers, can both reinforce soils and concretes and also may contribute to the protection of the environment [53].

Synthetic fibers are increasingly being used to reinforce soil. Jiang et al. [54] found that the 0.3% (by weight) polypropylene fiber is the optimal fiber percentage to increase the internal friction angle, cohesion, and UCS of soil. However, by increasing the fiber content

to above 0.3%, the abovementioned parameters were reduced. Consoli et al. [55] reported that an increase in fiber content, fiber aspect ratio, and fiber length improved the strength of the soil. However, by increasing the fiber diameter, the deviatoric stress decreased. Zaimoglu [56] concluded that, by increasing the polypropylene fiber content, the ductility of fiber-reinforced, fine-grained soils decreased significantly. Miller and Rifai [57] reported a reduction in the formation of cracks and hydraulic conductivity of compacted soil after using polypropylene fibers.

Stefanidou et al. [58] studied the effects of wood and cannabis, polypropylene, cellulose, and carbon fibers in pure lime mortars. Lime mortars reinforced with polypropylene and cannabis had a significantly higher amount of fracture energy compared to other mortars. The mechanical properties of wood-modified lime mortars improved by almost 25% in comparison to the reference sample; however, the cohesion of the matrix was problematic. Almerich et al. [59] used Glass Fiber-Reinforced Polymer (GFRP) bars as a replacement for steel bars in reinforced lime concrete. It was observed that the lime concrete modified with GFRP had high UCS, acceptable tensile strength, a higher elastic modulus and adhesion, good compatibility, and reduced cement alkalinity.

A review of the previous research studies indicated that there are limited studies available on the mechanical characteristics of lime-based concretes such as LCC, even though there are many studies available on lime–cement-stabilized soils, lime–hemp concrete and lime–cement mortars. Moreover, a comprehensive literature review by the authors demonstrated that, at present, there has been no research performed to evaluate the effect of polyamide fibers on the mechanical properties of LCC as a widely used, lime-based concrete in some warm regions. To address this research gap, LCC samples were prepared with different percentages of polyamide fibers and cured at different times at two different temperatures. Then, the effects of the fibers' contents, curing conditions, and curing periods on the mechanical properties of LCC, such as the deformability index, secant modulus, bulk modulus, shear modulus, stiffness ratio, strain energy, failure strain, strength ratio, and failure patterns, were investigated. Based on the test results, a simple mathematical model was also established to forecast the mechanical properties of polyamide fiber-reinforced LCC.

2. Raw Materials

The coarse aggregates utilized in the current study were well-graded sand with silt (SW-SM) that were sourced from a quarry in Iran, named Ekhtiarabad, where most of the coarse aggregates utilized in concreting projects in Kerman, a city in Iran, are sourced from. In most construction sites in Kerman, layers of fine-grained soils are found about 30 m beneath the ground surface. Therefore, the fine-grained soil utilized in the current work was sourced from a building site in Kerman, which can reasonably represent the soil properties that are available in most construction sites in Kerman. The sieve and hydrometer analysis test results and the engineering properties of the used soils are presented in Figure 1 and Table 1. In Table 1, D10 represents the diameter where 10% of the sample's mass consists of smaller particles. The uniformity coefficient (Cu) is determined by the ratio of D60 to D10. The coefficient of curvature (C_c) is given by the formula: $C_c = \frac{D30^2}{D60 \cdot D10}$. Additionally, the abbreviations PL, LL, and PI represent plastic limit, liquid limit, and plastic index, respectively. The chemical compositions of the materials were determined using X-ray Fluorescence (XRF) analysis using Bruker S_4-Explorer. As can be seen in Table 2, the clayey soil is mostly characterized by 41.75% SiO_2, 15.15% Al_2O_3, and 5.2% Fe_2O_3, which has a total share of 62.1% (lower than 70%, which is specified as the minimum requirement based on ASTM C618-15 [60]). Therefore, increasing the compressive strength and reducing the shrinkage and swelling properties of the soil could be achieved through the application of pozzolanic materials such as cement, lime, or a blend of cement and lime [5,61]. Table 2 shows that calcium oxide (CaO) is the main component of lime and that CaO and silica (SiO_2) are key components of cement. Similar types of materials were used in the authors' previous studies [13,15].
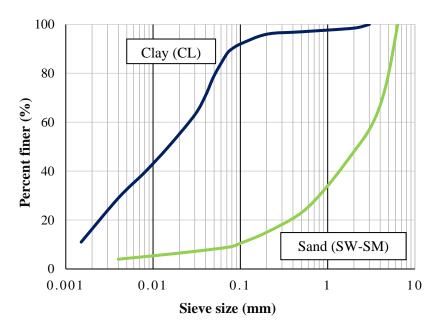
Figure 1. Sieve analysis of tested soils [15].

Table 1. Properties of tested soils.

Characteristics	Results	Used Standards
Coarse aggregates type	SW-SM	ASTM 2487-11 [62]
D_{10}	0.11	ASTM D422-63 [63]
C_u	33	ASTM D422-63 [63]
C^c	1.86	ASTM D422-63 [63]
PL	21%	ASTM D424-54 [64]
LL	26%	ASTM D423-66 [65]
PI	5%	Das 2019 [66]
Fine aggregates type	Cay (CL)	ASTM 2487-11 [67]
Mineral	Kaolinite	Das 2019 [66]
Activity degree	0.48	Das 2019 [66]
D_{10}	0.0016	ASTM D422-63 [63]
C_u	18	ASTM D422-63 [63]
C_C	0.40	ASTM D422-63 [63]
PL	23%	ASTM D424-54 [64]
LL	33%	ASTM D423-66 [65]
PI	10%	Das 2019 [66]
Optimum moisture	15%	AASHTO T180 [68]
Maximum specific weight	18.76 kN/m^3	AASHTO T180 [68]
Specific gravity (G_s)	2.46	ASTM D854-10 [69]
UCS	111.33 kPa	ASTM D2166 [70]

Table 2. Oxide compounds of cement, lime, and clay.

Component Oxides	Clay Composition (%)	Lime Composition (%)	Cement Composition (%)
Calcium oxide (CaO)	13.20	73.70	63.41
Silica (SiO$_2$)	41.75	1.15	21.66
Alumina (Al$_2$O$_3$)	15.15	0.11	4.21
Iron oxide (Fe$_2$O$_3$)	5.20	0.24	3.10
Magnesium oxide (MgO)	5.13	1.619	2.82
Sulfur trioxide (SO$_3$)	3.48	0.015	2.61
Chloride as NaCl	0.08	0.011	-
Manganese (Mn)	-	0.005	-
Loss on ignition	12.58	23.15	0.81

3. Methodology, Sample Preparation, and Testing

A total of 48 cylindrical LCC specimens were prepared with different fiber contents for different curing days and curing conditions. To increase the accuracy of the results, three (3) similar specimens were cast for each test, and the average testing results were calculated and reported.

Polyamide fibers are known to have ultrahigh tensile strength at low weight, a high melting point, and excellent heat and flame resistance as well as appropriate solvent resistance and dimensional stability at elevated and room temperatures.

Table 3 shows the mixture proportion, curing time, and curing condition for the different mixes. The percentages of cement and lime in all specimens were kept constant at 4% and 3% of the dry weight of the clay and coarse-grained soil mixtures, respectively. The water content was 24.04% of the total dry weight of the clay, coarse-grained soil, cement, and lime mixture; moreover, in all the specimens, the clay content was equal to 23% of the dry weight of coarse-grained soil. The fibers were added to the mixes at 0.5%, 1%, and 2% of the total dry weight of the coarse-grained soil, cement, lime, and clay mixture.

Table 3. Composition of LCC specimens.

Specimen	Clay Content (%)	Lime Content (%)	Cement Content (%)	Water Content (%)	Fiber Content (%)	Curing Temp. (°C)	Curing Time (Days)	Number of Samples	Curing Condition
* F0-7-L	23	3	4	24.04	0	20	7	3	Lab
F0.5-7-L	23	3	4	24.04	0.5	20	7	3	Lab
F1-7-L	23	3	4	24.04	1	20	7	3	Lab
F2-7-L	23	3	4	24.04	2	20	7	3	Lab
F0-28-L	23	3	4	24.04	0	20	28	3	Lab
F0.5-28-L	23	3	4	24.04	0.5	20	28	3	Lab
F1-28-L	23	3	4	24.04	1	20	28	3	Lab
F2-28-L	23	3	4	24.04	2	20	28	3	Lab
F0-3-O	23	3	4	24.04	0	50	3	3	Oven
F0.5-3-O	23	3	4	24.04	0.5	50	3	3	Oven
F1-3-O	23	3	4	24.04	1	50	3	3	Oven
F2-3-O	23	3	4	24.04	2	50	3	3	Oven
F0-7-O	23	3	4	24.04	0	50	7	3	Oven
F0.5-7-O	23	3	4	24.04	0.5	50	7	3	Oven
F1-7-O	23	3	4	24.04	1	50	7	3	Oven
F2-7-O	23	3	4	24.04	2	50	7	3	Oven

* Explanation of abbreviations: F(fiber content)-(curing days)-(curing condition); for example: F0-7-L = sample with 0% fiber and cured for 7 days in laboratory condition.

In order to prepare the LCC samples, coarse and fine aggregates were properly blended together. Then, a lime–cement slurry was made by blending lime and cement with optimum water content. Then, the mixture of coarse-grained and clay soils was added to the lime–cement slurry. The process of mixing continued until a homogeneous paste was attained. The fresh mixture was cast into several cylinders that were 60 mm in diameter and 120 mm in height. After 72 h of concrete casting, the samples were demolded and then placed in a plastic bag to avoid moisture loss. Half of the samples were oven-cured for 3 or 7 days at 50 °C, and the rest were cured for 7 or 28 days at an ambient temperature of 20 °C. The samples were then tested under uniaxial compression after curing because compressive strength is the most important factor in concrete design [71].
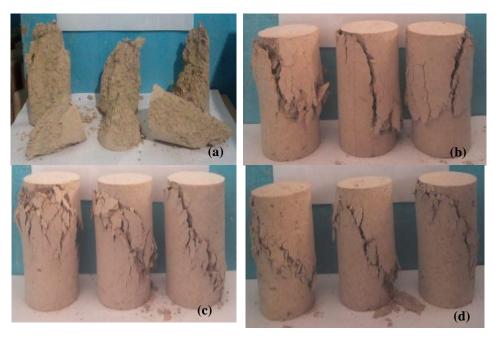
4. Results and Discussion

4.1. Failure Pattern

Figures 2 and 3 show the failure patterns of the control and LCC samples. The LCC without fibers had diagonal cracks and gradually expanded toward the middle of the sample. Therefore, the LCC surface clod spalled off, leading to a brittle failure. For the
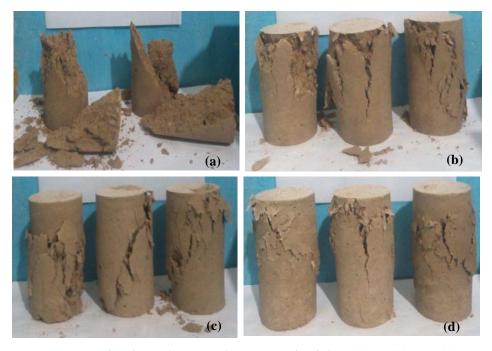
LCC samples with 0.5% or 1% fibers, the crack width became smaller with increasing fiber content. The uniformly dispersed fibers in the LCC created a mesh constraint on the soil particles. Thus, crack initiation and development were inhibited. By adding extra fibers (2%) to the LCC, the fibers agglomerated in it. This was due to the development of cracks in the LCC, destroying it gradually due to fiber agglomeration, i.e., when the frictional resistance between fibers is smaller compared with that between the fiber and soil particles. Duan and Zhang [72] have also reported a similar failure pattern.

Figure 2. A view of oven-cured specimens after failure: (**a**) 0%, (**b**) 0.5%, (**c**) 1%, and (**d**) 2% fiber content.

Figure 3. A view of 28-day, ambient-cured specimens after failure: (**a**) 0%, (**b**) 0.5%, (**c**) 1%, and (**d**) 2% fiber content.

4.2. Unconfined Compressive Strength and Stress–Strain Properties of Lime–Cement Concrete

The results of the UCS tests on the LCC specimens with fiber contents of 0%, 0.5%, 1%, and 2% cured at various times and conditions are shown in Figures 4 and 5. The results show that, by adding any percentage of fiber content, the UCS increased compared to the specimens without fibers. The tensile strength of fiber is high compared to concrete with a low tensile strength. Therefore, by adding fibers to concrete, the tensile force (relative movement of the particles) moves towards fibers and, ultimately, the strength increases. Irrespective of curing time and condition, specimens with 1% fibers achieved the highest UCS. The UCS for specimens F1-3-O, F1-7-O, F1-7-L, and F1-28-L increased by 25.4%, 15.9%, 19.2%, and 26.0% compared to the reference specimens without fibers.
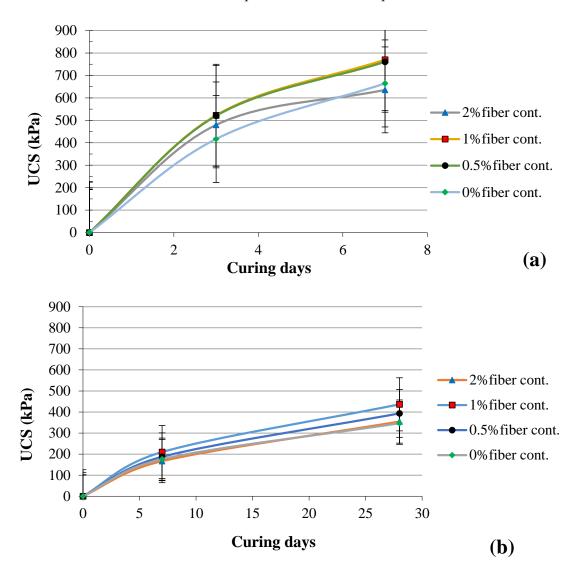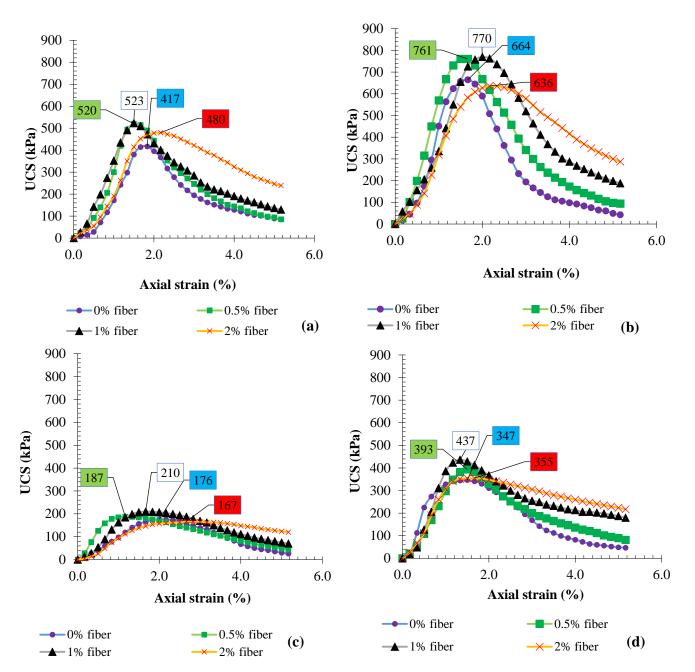

Figure 4. Peak UCS vs. curing time: (**a**) oven-cured samples, (**b**) ambient-cured samples.

The samples cured in an oven had higher UCS values compared with samples cured in an ambient condition. This is because hydration is enhanced in cementitious materials cured at high temperatures compared to ambient-cured materials [73–77]. The UCS of F1-7-O was more than 3.5 times that of F1-7-L. Therefore, by comparing the effects of all variables, it can be concluded that the curing condition has the highest impact on the UCS value. The significant impact of curing periods and saturation degrees on the compressive strength of LC has also been previously reported [13,15,78].

Figure 5. UCS vs. axial strain: (**a**) 3-day, oven-cured (3-O), (**b**) 7-day, oven-cured (7-O), (**c**) 7-day, lab-cured (7-L), (**d**) 28-day, lab-cured (28-L).

Saberian et al. [15] reported that the rate of increase in the UCS was negligible for specimens after a 28-day curing period. For instance, the UCS of LC at a 20% degree of saturation (S_r) in the first 28 days increased from 0 kPa to 259 kPa; however, in the next 32 days, it showed a further increase to 290 kPa. It was found that 89% of the maximum strength was achieved in the first 28 days. In the current study, all specimens achieved 68% of their 7-day strength in the first 3 days of their curing time in oven conditions; however, at ambient conditions, they only achieved 48% of their 28-day strength in the first 7 days of their curing time (see Figure 4).

Based on the experimental results shown in Figures 4 and 5, the relationships between UCS and the fiber content of the LCC specimens at different curing conditions and curing days were developed and summarized in Figure 6.
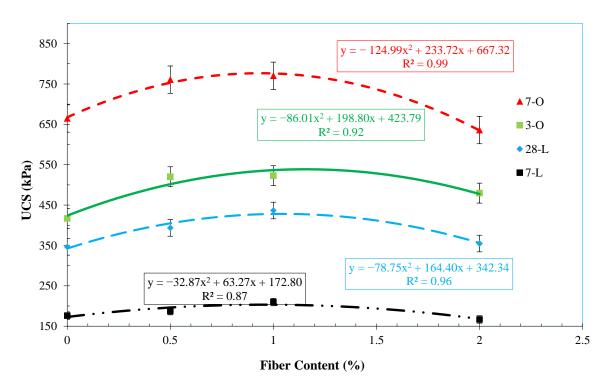
Figure 6. Relationship between UCS and fiber content at different curing conditions and curing days.

4.3. Mechanical Properties of Lime–Cement Concrete

A number of the mechanical properties of the LCC samples, including the failure strain, secant modulus (E_s), deformability index (I_d), resilient modulus (M_r), strain energy (SE), brittleness index (I_b), bulk modulus (K), shear modulus (G_s), strength ratio (R_{qu}), and the stiffness ratio (R_{Eu}) of specimens at different curing times, were determined by using the following equations and are summarized in Tables 4 and 5.

Table 4. Mechanical characteristics of oven-cured lime–cement concrete.

FC (%)	Curing Days	UCS (kPa)	ε_f (%)	E_s (MPa)	I_d	I_b	SE (kPa)	K (MPa)	G_s (MPa)	M_r (MPa)	R_{qu}	R_{Eu}
0	3	417	0.87	42	1.00	1.00	11	35	16	120	1.00	1.00
0.5	3	520	1.30	49	1.50	0.75	11	41	19	133	1.25	1.17
1	3	523	1.50	42	1.73	0.73	14	35	16	134	1.25	1.00
2	3	480	1.70	36	1.96	0.66	16	30	14	128	1.15	0.86
0	7	664	1.12	95	1.00	1.00	15	79	37	151	1.00	1.00
0.5	7	761	1.30	74	1.16	0.94	18	62	26	163	1.14	1.16
1	7	770	1.55	43	1.38	0.80	20	36	17	164	1.16	1.38
2	7	636	2.00	48	1.79	0.73	21	40	18	148	0.96	1.79

Table 5. Mechanical characteristics of ambient-cured lime–cement concrete.

FC (%)	Curing Days	UCS (kPa)	ε_f (%)	E_s (MPa)	I_d	I_b	SE (kPa)	K (MPa)	G_s (MPa)	M_r (MPa)	R_{qu}	R_{Eu}
0	7	176	1.83	12.14	1.00	1.00	4.87	10.12	5	91	1.00	1.00
0.5	7	187	1.06	29.26	0.58	0.78	6.15	24.38	11	92	1.06	2.41
1	7	210	1.29	21.73	0.70	0.67	7.00	18.11	8	95	1.19	1.79
2	7	167	1.44	12.18	0.79	0.61	7.16	10.15	5	89	0.95	1.00
0	28	347	1.92	66.13	1.00	1.00	9.51	55.11	25	112	1.00	1.00
0.5	28	393	1.00	35.89	0.52	0.83	10.35	29.91	14	118	1.14	0.54
1	28	437	1.03	52.46	0.54	0.83	11.57	43.72	20	123	1.26	0.79
2	28	355	1.17	45.04	0.61	0.79	13.67	37.53	17	113	1.02	0.68

The secant modulus was used to evaluate LCC resistance to deformation, which was determined from the UCS test results using Equation (1) [79].

$$E_S = \frac{\Delta\sigma}{\Delta\varepsilon} = \frac{\sigma_2 - \sigma_1}{\varepsilon_2 - \varepsilon_1} \tag{1}$$

where σ_2 is maximum stress in the elastic stage and σ_1 is minimum stress in the elastic stage; ε_1 and ε_2 are corresponding strains of σ_1 and σ_2.

The deformability index (I_D) is obtained from Equation (2) for measuring the deformation, brittleness, and ductility of soils and rocks [1,2].

$$I_D = \frac{\varepsilon_{ct}}{\varepsilon_{cu}} \tag{2}$$

where ε_{ct} is the axial strain at the maximum UCS of unreinforced LCC specimens (with 0% fiber content) and ε_{cu} is the axial strain at the maximum UCS of the fiber-reinforced LCC specimens.

The resilient modulus (M_r) is a measure of the soil elastic response under stress (AASHTO Test Method T307 2005), which is expressed as [3]:

$$M_r(MPa) = 0.124 \times UCS(kPa) + 68.8 \tag{3}$$

Bulk modulus (K) is the ratio of change in overall stress to the change in volumetric strain [80,81], which is determined as:

$$K = \frac{\sigma}{\frac{\Delta V}{V}} = \frac{\sigma}{\varepsilon_{xx} + \varepsilon_{yy} + \varepsilon_{zz}} = \frac{E_s}{3(1 - 2\vartheta)} \tag{4}$$

where $\frac{\Delta V}{V}$ is the relative volume change, σ is hydrostatic pressure, ε_{xx}, ε_{yy}, and ε_{zz} are direct strains, and υ is Poisson's ratio [81].

Shear modulus was measured using the following equation [82]:

$$G(MPa) = \frac{\sigma_{xy}}{(\varepsilon_{xy} + \varepsilon_{yx})} = \frac{\sigma_{xy}}{2\varepsilon_{xy}} = \frac{\sigma_{xy}}{\gamma_{xy}} = \frac{E_s(kPa)}{2(1 + \vartheta)} = \frac{E_s(kPa)}{3} \tag{5}$$

where σ_{xy} is shear stress, ε is shear strain, and $\gamma_{xy} = \varepsilon_{xy} + \varepsilon_{yx} = 2\varepsilon_{xy}$ [82].

Strain energy was measured as the area under the stress–strain curve [83,84]. The stiffness ratio and strength ratio for measuring the effects of fiber content (FC) on the stress–strain behavior of the soil and the failure mechanisms were obtained using Equations (6) and (7):

$$R_{q_u} = \frac{UCS_{(FC \neq 0)}}{UCS_{(FC = 0)}} \tag{6}$$

$$R_{E_u} = \frac{E_{s(FC \neq 0)}}{E_{s(FC = 0)}} \tag{7}$$

where UCS is the maximum unconfined compressive strength and Es is secant Young's modulus, which is the slope of the linear part of the stress–strain curve.

The brittleness index (I_b) is an indicator for the classification of soil strain softening severity and contractiveness. The brittleness index was determined using Equation (8) by calculating the variance between the peak and critical undrained shear strengths that are normalized by the peak undrained strength.
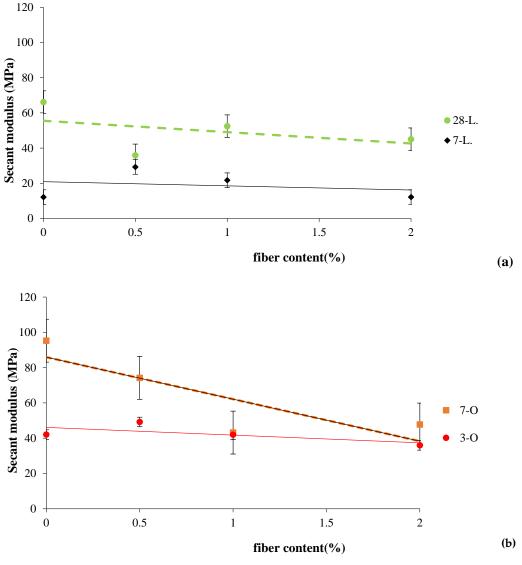
$$I_b = \frac{q_p - q_r}{q_p} \tag{8}$$

where q_p is the peak stress and q_r is the critical undrained shear strength obtained from UCS curves.

The results provided in Tables 4 and 5 show the relationship between the strain energy (energy absorption of LCC samples) and fiber content of samples cured for different days at both curing conditions. The testing outcomes show that an increase in the fiber content increased the area under the stress–strain curve. This effect can be seen in all specimens with different curing times and curing conditions. The strain energies of LCC specimens containing 0.5%, 1%, and 2% fiber contents in 3-day, oven-curing conditions increased by 6.54%, 35.73%, and 52.70%, respectively. This is because, by adding fibers to LCC specimens, the flexibility increased and the samples could resist greater strains.

Figure 7 shows the secant modulus versus the fiber content at different curing periods for ambient-cured and oven-cured samples, respectively. The results show that, at any curing time and curing condition, by increasing the fiber content, the secant modulus decreased because the contact behaviors between the cement and soil particles were decreased by the addition of fiber. This finding agrees with the conclusions drawn in previous studies [72,79,85,86].

(a)

(b)

Figure 7. Relationship between secant modulus and fiber content of the LCC specimens in (**a**) ambient-curing and (**b**) oven-curing conditions.
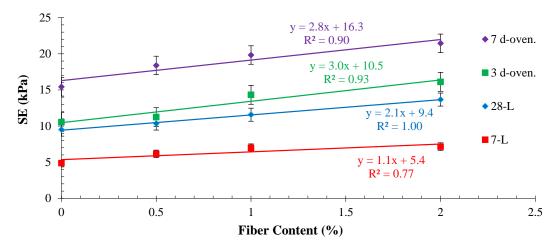
Figure 8 shows the deformability index versus fiber content at different curing conditions. For samples under 3-day, oven-cured and 7-day, ambient-cured conditions, by increasing the fiber content, the deformability index increased. However, for specimens under the 7-day, oven-cured and 28-day, ambient-cured conditions, the deformability index increased by increasing the fiber content from 0% to 0.5%; moreover, it remained constant due to an increase in the fiber content from 0.5% to 2%. Therefore, using more than 0.5% fiber content did not affect the deformability index of the LCC specimens. The deformability of the fiber-reinforced LCC specimens increased regardless of the curing period and curing condition because the fiber increased the flexibility and deformability of the specimens.

Figure 8. Relationship between deformability index and fiber content of specimens with different curing times and conditions.

According to Figure 9, it can be seen that with an increase in the amount of fibers and the age of the samples, the area under the stress-strain diagram, which is the energy absorbed by the material, is increased. Also, increasing the curing temperature is an important factor that increases the ability of materials to absorb energy. As can be seen in Figure 9, the samples that were cured at a higher temperature had a greater ability to absorb energy than the samples that were cured at the laboratory temperature. In other words, the ability of the samples to absorb energy was increased with increasing the curing temperature, age and fiber content.

Figure 9. Relationship between strain energy and fiber content of specimens with different curing times and conditions.
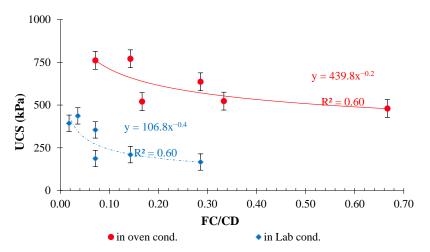
5. Mathematical (Phenomenological) Model

According to the UCS test results, the mechanical properties of the LCC samples were affected significantly by the fiber content, curing condition, and curing time. Saberian et al. [4,15] and Cong et al. [87] used the power function expressed by Equation (9) to predict the results as this function provides excellent matches between the experimental and predicted results. Similar to Equation (9), a power function was introduced in the current study to predict the experimental results. In the proposed model, FC is the percentage of fiber content and CD is number of curing days. The brittleness index, deformability index, secant modulus, bulk modulus, resilient modulus, and shear modulus of fiber-reinforced LCC specimens, as well as the parameter of the FC/CD, were variables for predicting UCS.
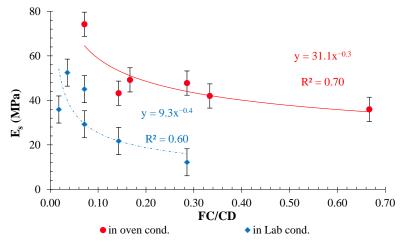
$$UCS = a \times C^b \tag{9}$$

where C is equal to FC/CD; a and b (dimensionless parameter) are fitting parameters.

Based on the testing outcomes presented in Tables 4 and 5 and Equation (8), Figures 10–15 present the fitted curves for the relationships of compressive strength, E_s, K, G_s, M_r, and I_b versus the FC/CD of the LCC specimens. It can be seen that the fitted curves in Figures 10–15 have good accuracy.
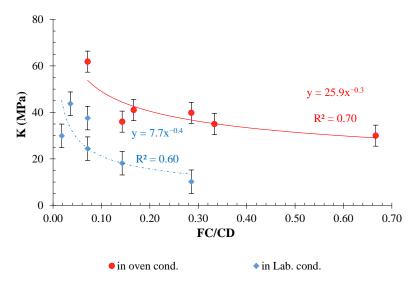

Figure 10. Fitted curves of UCS development as a function of FC/CD in oven- and ambient-cured conditions.
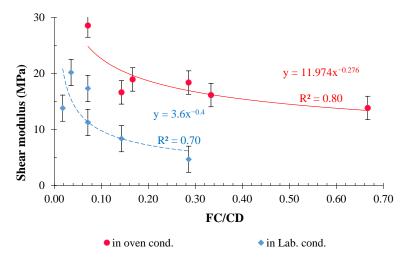

Figure 11. Fitted curves of Es development as a function of FC/CD in oven- and ambient-cured conditions.
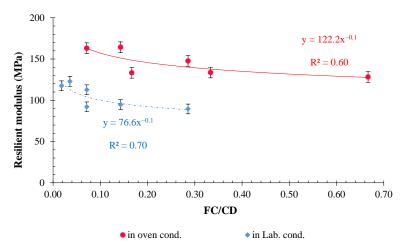
Figure 12. Fitted curves of bulk modulus development as a function of FC/CD in oven- and ambient-cured conditions.
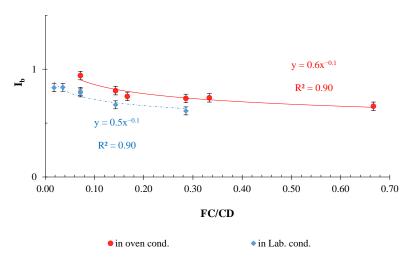

Figure 13. Fitted curves of G_s development as a function of FC/CD in oven- and ambient-cured conditions.

Figure 14. Fitted curves of resilient modulus development as a function of FC/CD in oven- and ambient-cured conditions.

Figure 15. Fitted curves of brittleness index development as a function of FC/CD in oven- and ambient-cured conditions.

6. Conclusions

This research investigated the effects of curing times, curing conditions, and polyamide fiber contents on the mechanical characteristics of lime–cement concrete (LCC). According to the findings, the conclusions are summarized below:

- The optimum fiber content to increase the UCS of LCC is 1%. Increasing the fiber content from 1% to 2% led to a decrease in the UCS due to a reduction in cohesion;
- The energy absorption in LCC increased with increasing fiber content. In addition, LCC with a higher fiber content (i.e., over 1%) showed more ductile post-peak behavior compared to LCC with a lower fiber content;
- Curing times and conditions have significant effects on UCS values. Specimens cured in oven conditions showed higher UCS values compared to the ambient-cured specimens;
- The application of polyamide fibers, in general, showed a positive impact on improving the mechanical properties of LCC. However, the secant modulus of specimens for any curing condition and curing period decreased by increasing the fiber content;
- The deformability index of specimens for any curing condition and curing period increased by increasing the fiber content;
- Based on the laboratory test results, simple models were developed to predict the mechanical properties of LCC samples in relation to fiber content and curing days. Their prediction accuracy is reasonably good.

It is recommended that future studies be conducted to study the impact of fiber content on the flexural strength and workability of LCC specimens. Also, the durability of the fiber-reinforced LCC samples in exposure to wetting–drying and freezing–thawing conditions can be investigated.

Institutional Review Board Statement: Not applicable.

Informed Consent Statement: Not applicable.

Conflicts of Interest: The authors declare no conflict of interest.

References

1. Islam, M.S.; Hashim, R. Bearing Capacity of Stabilised Tropical Peat by Deep Mixing Method. *Aust. J. Basic Appl. Sci.* **2009**, *3*, 682–688.

2. Al-Swaidani, A.; Hammoud, I.; Meziab, A. Effect of Adding Natural Pozzolana on Geotechnical Properties of Lime-Stabilized Clayey Soil. *J. Rock Mech. Geotech. Eng.* **2016**, *8*, 714–725. [CrossRef]

3. Umar, M.; Kassim, K.A.; Chiet, K.T.P. Biological Process of Soil Improvement in Civil Engineering: A Review. *J. Rock Mech. Geotech. Eng.* **2016**, *8*, 767–774. [CrossRef]

4. Saberian, M.; Khabiri, M.M. Effect of Oil Pollution on Function of Sandy Soils in Protected Deserts and Investigation of Their Improvement Guidelines (case Study: Kalmand Area, Iran). *Environ. Geochem. Health* **2018**, *40*, 243–254. [CrossRef] [PubMed]

5. Zainorabidin, A.; Wijeyesekera, D.C. Geotechnical Challenges with Malaysian Peat. 2007. Available online: https://repository. uel.ac.uk/download/41d7bd3a3df6b74d6069261c0817e0b8f3d7dad24a5ff57f5dc3af0e34011ad3/363072/Zainorabidin%2C%20 A%20%282007%29%20AC%26T%20252-61.pdf (accessed on 13 April 2023).

6. Puppala, A.J.; Musenda, C. Effects of Fiber Reinforcement on Strength and Volume Change in Expansive Soils. *Transp. Res. Rec.* **2000**, *1736*, 134–140. [CrossRef]

7. Saberian, M.; Rahgozar, M.A. Geotechnical Properties of Peat Soil Stabilised with Shredded Waste Tyre Chips in Combination with Gypsum, Lime or Cement. *Mires Peat* **2016**, *18*, 1–16. [CrossRef]

8. Rogers, C.D.; Boardman, D.I.; Papadimitriou, G. Stress Path Testing of Realistically Cured Lime and Lime/cement Stabilized Clay. *J. Mater. Civ. Eng.* **2006**, *18*, 259–266. [CrossRef]

9. Thyagaraj, T.; Zodinsanga, S. Swell–shrink Behaviour of Lime Precipitation Treated Soil. *Proc. Inst. Civ. Eng. Improv.* **2014**, *167*, 260–273. [CrossRef]

10. Jahandari, S. *Laboratory Study of Moisture and Capillarity Impact on Lime Concrete Resistance due to the Increase of Ground Water Level*; Faculty of Civil and Surveying Engineering, Department of Geotechnical Engineering, Graduate University of Advanced Technology: Kerman, Iran, 2015.

11. Ameri, M.; Kalantari, B.; Jahandari, S. Laboratory Study of Determination of Optimum Amount of Water and Clay in Mortar Made with Lime and Fly Ash. In Proceedings of the International Conference on Research in Science and Technology, Kualalumpur, Malaysia, 14 December 2015.

12. Jahandari, S.; Saberian, M.; Zivari, F.; Li, J.; Ghasemi, M.; Vali, R. Experimental Study of the Effects of Curing Time on Geotechnical Properties of Stabilized Clay with Lime and Geogrid. *Int. J. Geotech. Eng.* **2019**, *13*, 172–183. [CrossRef]

13. Jahandari, S.; Toufigh, M.M.; Li, J.; Saberian, M. Laboratory Study of the Effect of Degrees of Saturation on Lime Concrete Resistance due to the Groundwater Level Increment. *Geotech. Geol. Eng.* **2018**, *36*, 413–424. [CrossRef]

14. Jahandari, S.; Li, J.; Saberian, M.; Shahsavarigoughari, M. Experimental Study of the Effects of Geogrids on Elasticity Modulus, Brittleness, Strength, and Stress-Strain Behavior of Lime Stabilized Kaolinitic Clay. *GeoResJ* **2017**, *13*, 49–58. [CrossRef]

15. Saberian, M.; Jahandari, S.; Li, J.; Zivari, F. Effect of Curing, Capillary Action, and Groundwater Level Increment on Geotechnical Properties of Lime Concrete: Experimental and Prediction Studies. *J. Rock Mech. Geotech. Eng.* **2017**, *9*, 638–647. [CrossRef]

16. Firoozfar, A.; Khosroshiri, N. Kerman Clay Improvement by Lime and Bentonite to Be Used as Materials of Landfill Liner. *Geotech. Geol. Eng.* **2017**, *35*, 559–571. [CrossRef]

17. Costigan, A.; Pavía, S.; Kinnane, O. An Experimental Evaluation of Prediction Models for the Mechanical Behavior of Unreinforced, Lime-Mortar Masonry under Compression. *J. Build. Eng.* **2015**, *4*, 283–294. [CrossRef]

18. Pavlík, V.; Užáková, M. Effect of Curing Conditions on the Properties of Lime, Lime–metakaolin and Lime–zeolite Mortars. *Constr. Build. Mater.* **2016**, *102*, 14–25. [CrossRef]

19. de Bruijn, P.B.; Jeppsson, K.-H.; Sandin, K.; Nilsson, C. Mechanical Properties of Lime–hemp Concrete Containing Shives and Fibres. *Biosyst. Eng.* **2009**, *103*, 474–479. [CrossRef]

20. Walker, R.; Pavia, S.; Mitchell, R. Mechanical Properties and Durability of Hemp-Lime Concretes. *Constr. Build. Mater.* **2014**, *61*, 340–348. [CrossRef]

21. Thyagaraj, T.; Samuel, Z.; Kumar, K.S.R. Relative Efficiencies of Electrolytes in Stabilization of an Expansive Soil. *Int. J. Geotech. Eng.* **2016**, *10*, 107–113. [CrossRef]

22. Bartlett, S.; Farnsworth, C. Performance of Lime Cement-Stabilized Soils for the I-15 Reconstruction Project: Salt Lake City, Utah. *Transp. Res. Rec.* **2002**, *1808*, 58–66. [CrossRef]

23. Chand, S.K.; Subbarao, C. Strength and Slake Durability of Lime Stabilized Pond Ash. *J. Mater. Civ. Eng.* **2007**, *19*, 601–608. [CrossRef]

24. Malekpoor, M.; Toufigh, M. Laboratory Study of Soft Soil Improvement Using Lime Mortar-(well Graded) Soil Columns. *Geotech. Test. J.* **2010**, *33*, 225–235.

25. Toohey, N.M.; Mooney, M.A.; Bearce, R.G. Stress-Strain-Strength Behavior of Lime-Stabilized Soils during Accelerated Curing. *J. Mater. Civ. Eng.* **2013**, *25*, 1880–1886. [CrossRef]

26. Pakravan, H.R.; Ozbakkaloglu, T. Synthetic Fibers for Cementitious Composites: A Critical and in-Depth Review of Recent Advances. *Constr. Build. Mater.* **2019**, *207*, 491–518. [CrossRef]

27. Wang, L.; Tang, S. High-Performance Fiber-Reinforced Composites: Latest Advances and Prospects. *Buildings* **2023**, *13*, 1094. [CrossRef]

28. Wang, L.; Tang, S.; Chen, T.E.; Li, W.; Gunasekara, C. Sustainable High-Performance Hydraulic Concrete. *Sustainability* **2022**, *14*, 695. [CrossRef]

29. Wang, L.; Tang, S. High-Performance Construction Materials: Latest Advances and Prospects. *Buildings* **2022**, *12*, 928. [CrossRef]

30. Maher, M.H.; Ho, Y.C. Behavior of Fiber-Reinforced Cemented Sand under Static and Cyclic Loads. *Geotech. Test. J.* **1993**, *16*, 330–338.

31. Omine, K.; Ochiai, H.; Yasufuku, N.; Kato, T. Effect of Plastic Wastes in Improving Cement-Treated Soils. *Proc. 2nd Int. Congr. Environ. Geotech.* **1996**, 875–880.

32. Prabakar, J.; Sridhar, R.S. Effect of Random Inclusion of Sisal Fibre on Strength Behaviour of Soil. *Constr. Build. Mater.* **2002**, *16*, 123–131. [CrossRef]

33. Michalowski, R.L.; Čermák, J. Triaxial Compression of Sand Reinforced with Fibers. *J. Geotech. Geoenviron. Eng.* **2003**, *129*, 125–136. [CrossRef]

34. Cai, Y.; Shi, B.; Ng, C.W.W.; Tang, C.S. Effect of Polypropylene Fibre and Lime Admixture on Engineering Properties of Clayey Soil. *Eng. Geol.* **2006**, *87*, 230–240. [CrossRef]

35. Miraftab, M.; Lickfold, A. Utilization of Carpet Waste in Reinforcement of Substandard Soils. *J. Ind. Text.* **2008**, *38*, 167–174. [CrossRef]

36. Lovisa, J.; Shukla, S.K.; Sivakugan, N. Behaviour of Prestressed Geotextile-Reinforced Sand Bed Supporting a Loaded Circular Footing. *Geotext. Geomembr.* **2010**, *28*, 23–32. [CrossRef]

37. Mandal, J.N.; Murthi, M.V.R. Potential Use of Natural Fibres in Geotechnical Engineering. In Proceedings of the International Workshops on Geo-Textiles, Bangalore, India, 22 November 1989; pp. 22–29.

38. Sivakumar Babu, G.L.; Vasudevan, A.K. Strength and Stiffness Response of Coir Fiber-Reinforced Tropical Soil. *J. Mater. Civ. Eng.* **2008**, *20*, 571–577. [CrossRef]

39. Dang, L.C.; Fatahi, B.; Khabbaz, H. Behaviour of Expansive Soils Stabilized with Hydrated Lime and Bagasse Fibres. *Procedia Eng.* **2016**, *143*, 658–665. [CrossRef]

40. Kafodya, I.; Okonta, F. Effects of Natural Fiber Inclusions and Pre-Compression on the Strength Properties of Lime-Fly Ash Stabilised Soil. *Constr. Build. Mater.* **2018**, *170*, 737–746. [CrossRef]

41. Yixian, W.; Panpan, G.; Shengbiao, S.; Haiping, Y.; Binxiang, Y. Study on Strength Influence Mechanism of Fiber-Reinforced Expansive Soil Using Jute. *Geotech. Geol. Eng.* **2016**, *34*, 1079–1088. [CrossRef]

42. Azadegan, O.; Kaffash, E.A.; Yaghoubi, M.J.; Pourebrahim, G.R. Laboratory Study on the Swelling, Cracking and Mechanical Characteristics of the Palm Fiber Reinforced Clay. *Electron. J. Geotech. Eng.* **2012**, *17*, 47–54.

43. Akbulut, S.; Arasan, S.; Kalkan, E. Modification of Clayey Soils Using Scrap Tire Rubber and Synthetic Fibers. *Appl. Clay Sci.* **2007**, *38*, 23–32. [CrossRef]

44. Consoli, N.C.; Montardo, J.P.; Donato, M.; Prietto, P.D. Effect of Material Properties on the Behaviour of Sand—Cement—Fibre Composites. *Proc. Inst. Civ. Eng. Improv.* **2004**, *8*, 77–90. [CrossRef]

45. Chaduvula, U.; Viswanadham, B.V.S.; Kodikara, J. A Study on Desiccation Cracking Behavior of Polyester Fiber-Reinforced Expansive Clay. *Appl. Clay Sci.* **2017**, *142*, 163–172. [CrossRef]

46. Consoli, N.C.; Prietto, P.D.; Ulbrich, L.A. Influence of Fiber and Cement Addition on Behavior of Sandy Soil. *J. Geotech. Geoenviron. Eng.* **1998**, *124*, 1211–1214. [CrossRef]

47. Mukherjee, K.; Mishra, A.K. Hydro-Mechanical Properties of Sand-Bentonite-Glass Fiber Composite for Landfill Application. *KSCE J. Civ. Eng.* **2019**, *23*, 4631–4640. [CrossRef]

48. Patel, S.K.; Singh, B. Strength and Deformation Behavior of Fiber-Reinforced Cohesive Soil under Varying Moisture and Compaction States. *Geotech. Geol. Eng.* **2017**, *35*, 1767–1781. [CrossRef]

49. Gao, L.; Zhou, Q.; Yu, X.; Wu, K.; Mahfouz, A.H. Experimental Study on the Unconfined Compressive Strength of Carbon Fiber Reinforced Clay Soil. *Mar. Georesources Geotechnol.* **2017**, *35*, 143–148. [CrossRef]

50. Cui, H.; Jin, Z.; Bao, X.; Tang, W.; Dong, B. Effect of Carbon Fiber and Nanosilica on Shear Properties of Silty Soil and the Mechanisms. *Constr. Build. Mater.* **2018**, *189*, 286–295. [CrossRef]

51. Fatahi, B.; Khabbaz, H.; Fatahi, B. Mechanical Characteristics of Soft Clay Treated with Fibre and Cement. *Geosynth. Int.* **2012**, *19*, 252–262. [CrossRef]

52. Hejazi, S.M.; Sheikhzadeh, M.; Abtahi, S.M.; Zadhoush, A. A Simple Review of Soil Reinforcement by Using Natural and Synthetic Fibers. *Constr. Build. Mater.* **2012**, *30*, 100–116. [CrossRef]

53. Valipour, M.; Shourijeh, P.T.; Mohammadinia, A. Application of Recycled Tire Polymer Fibers and Glass Fibers for Clay Reinforcement. *Transp. Geotech.* **2021**, *27*, 100474. [CrossRef]

54. Jiang, H.; Cai, Y.; Liu, J. Engineering Properties of Soils Reinforced by Short Discrete Polypropylene Fiber. *J. Mater. Civ. Eng.* **2010**, *22*, 1315–1322. [CrossRef]

55. Consoli, N.C.; Vendruscolo, M.A.; Prietto, P.D.M. Behavior of Plate Load Tests on Soil Layers Improved with Cement and Fiber. *J. Geotech. Geoenviron. Eng.* **2003**, *129*, 96–101. [CrossRef]

56. Zaimoglu, A.S. Freezing–thawing Behavior of Fine-Grained Soils Reinforced with Polypropylene Fibers. *Cold Reg. Sci. Technol.* **2010**, *60*, 63–65. [CrossRef]

57. Miller, C.J.; Rifai, S. Fiber Reinforcement for Waste Containment Soil Liners. *J. Env. Eng.* **2004**, *130*, 891–895. [CrossRef]

58. Papayianni, I.; Stefanidou, M.; Pachta, V. Plastering the Prehistory: Marl as a unique material to cover, maintain and decorate the Neolithic walls of Catalhöyük. In Proceedings of the 4th Historic Mortars Conference HMC2016, Santorini, Greece, 10–12 October 2016.

59. Almerich-Chulia, A.; Fenollosa, E.; Martin, P. Reinforced Lime Concrete with FRP: An Alternative in the Restoration of Architectural Heritage. *Appl. Mech. Mater.* **2016**, *851*, 751–756. [CrossRef]

60. *ASTM C 618-19*; Standard Specification for Mortar for Coal Fly Ash and Raw or Calcined Natural Pozzolan for Use in Concrete. ASTM International: West Conshohocken, PA, USA, 2015.

61. Sirivitmaitrie, C.; Puppala, A.J.; Saride, S.; Hoyos, L. Combined Lime–cement Stabilization for Longer Life of Low-Volume Roads. *Transp. Res. Rec.* **2011**, *2204*, 140–147. [CrossRef]

62. *ASTM D 2487-06*; Standard Practice for Classification of Soils for Engineering Purposes (Unified Soil). ASTM International: West Conshohocken, PA, USA, 2010.

63. *ASTM D422-63*; Standard Method for Particle-Analysis of Soils. ASTM International: West Conshohocken, PA, USA, 2002.

64. *ASTM-D424-54*; Standard Method of Test for Plastic Limit. ASTM International: West Conshohocken, PA, USA, 1982.

65. *ASTM D423-66*; Standard Test Method for Liquid Limit of Soils. ASTM International: West Conshohocken, PA, USA, 1982.

66. Das, B.M. *Advanced Soil Mechanics*; CRC press: Boca Raton, FL, USA, 2019; ISBN 1351215167.

67. *ASTM D2487-17*; Standard Practice for Classification of Soils for Engineering Purposes (Unified Soil Classification System) 1. ASTM International: West Conshohocken, PA, USA, 2017.

68. *AASHTO T 180-10*; Standard Method of Test for Moisture-Density Relations of Soils Using a 4.54-Kg (10-Lb) Rammer and a 457-Mm (18-In.) Drop. American Association of State Highway and Transportation Officials: Washington, DC, USA, 2010.

69. *ASTM D 854-1*; Standard Test Methods for Specific Gravity of Soil Solids by Water Pycnometer. ASTM International: West Conshohocken, PA, USA, 2010.

70. *ASTM D 2166*; Standard Test Method for Unconfined Compressive Strength of Cohesive Soil. ASTM International: West Conshohocken, PA, USA, 2016.

71. Piro, N.S.; Mohammed, A.; Hamad, S.M.; Kurda, R. Artificial Neural Networks (ANN), MARS, and Adaptive Network-Based Fuzzy Inference System (ANFIS) to Predict the Stress at the Failure of Concrete with Waste Steel Slag Coarse Aggregate Replacement. *Neural Comput. Appl.* **2023**, *35*, 13293–13319. [CrossRef]

72. Duan, X.; Zhang, J. Mechanical Properties, Failure Mode, and Microstructure of Soil-Cement Modified with Fly Ash and Polypropylene Fiber. *Adv. Mater. Sci. Eng.* **2019**, *2019*, 9561794. [CrossRef]

73. Elkhadiri, I.; Palacios, M.; Puertas, F. *Effect of Curing Temperatura on Hydration Process of Different Cement*; Czech Academy of Sciences: Staré Město, Czech Republic, 2009.

74. Price, W.H. Factors Influencing Concrete Strength. *J. Proc.* **1951**, *47*, 417–432. [CrossRef]

75. Escalante-Garcıa, J.I.; Sharp, J.H. The Microstructure and Mechanical Properties of Blended Cements Hydrated at Various Temperatures. *Cem. Concr. Res.* **2001**, *31*, 695–702. [CrossRef]

76. Lothenbach, B.; Winnefeld, F.; Alder, C.; Wieland, E.; Lunk, P. Effect of Temperature on the Pore Solution, Microstructure and Hydration Products of Portland Cement Pastes. *Cem. Concr. Res.* **2007**, *37*, 483–491. [CrossRef]

77. Ballester, P.; Hidalgo, A.; Mármol, I.; Morales, J.; Sánchez, L. Effect of Brief Heat-Curing on Microstructure and Mechanical Properties in Fresh Cement Based Mortars. *Cem. Concr. Res.* **2009**, *39*, 573–579. [CrossRef]

78. Jahandari, S.; Saberian, M.; Tao, Z.; Mojtahedi, S.F.; Li, J.; Ghasemi, M.; Rezvani, S.S.; Li, W. Effects of Saturation Degrees, Freezing-Thawing, and Curing on Geotechnical Properties of Lime and Lime-Cement Concretes. *Cold Reg. Sci. Technol.* **2019**, *160*, 242–251. [CrossRef]

79. Tang, L.; Cong, S.; Geng, L.; Ling, X.; Gan, F. The Effect of Freeze-Thaw Cycling on the Mechanical Properties of Expansive Soils. *Cold Reg. Sci. Technol.* **2018**, *145*, 197–207. [CrossRef]

80. Duncan, J.M.; Bursey, A. Soil Modulus Correlations. In *Foundation Engineering in the Face of Uncertainty: Honoring Fred H. Kulhawy*; American Society of Civil Engineers: Reston, VA, USA, 2013; pp. 321–336.

81. Hobbs, D.W. The Dependence of the Bulk Modulus, Young's Modulus, Creep, Shrinkage and Thermal Expansion of Concrete upon Aggregate Volume Concentration. *Matériaux Constr.* **1971**, *4*, 107–114. [CrossRef]

82. Selvadurai, A.P.S.; Katebi, A. Mindlin's Problem for an Incompressible Elastic Half-Space with an Exponential Variation in the Linear Elastic Shear Modulus. *Int. J. Eng. Sci.* **2013**, *65*, 9–21. [CrossRef]

83. Ostadan, F.; Ostadan, F.; Arango, I. *Energy-Based Method for Liquefaction Potential Evaluation, Phase I-Feasibility Study*; US Department of Commerce, National Institute of Standards and Technology: Gaithersburg, MD, USA, 1996.

84. Green, R.A.; Mitchell, J.K.; Polito, C.P. An Energy-Based Excess Pore Pressure Generation Model for Cohesionless Soils. In *Proceedings of the John Booker Memorial Symposium, Sydney, Australia*; AA Balkema Publishers: Rotterdam, The Netherlands, 2000; Volume 3.

85. Ding, M.; Zhang, F.; Ling, X.; Lin, B. Effects of Freeze-Thaw Cycles on Mechanical Properties of Polypropylene Fiber and Cement Stabilized Clay. *Cold Reg. Sci. Technol.* **2018**, *154*, 155–165. [CrossRef]

86. Li, L.; Shao, W.; Li, Y.; Cetin, B. Effects of Climatic Factors on Mechanical Properties of Cement and Fiber Reinforced Clays. *Geotech. Geol. Eng.* **2015**, *33*, 537–548. [CrossRef]

87. Cong, M.; Longzhu, C.; Bing, C. Analysis of Strength Development in Soft Clay Stabilized with Cement-Based Stabilizer. *Constr. Build. Mater.* **2014**, *71*, 354–362. [CrossRef]